doi:10.2533/chimia.2011.334 Chimia 65 (2011) 334–338

Accelerating Calculations of Ultrafast Time-Resolved Electronic Spectra with Efficient Quantum Dynamics Methods

Marius Wehrle, Miroslav Šulc, and Jiří Vaníček*

Abstract: We explore three specific approaches for speeding up the calculation of quantum time correlation functions needed for time-resolved electronic spectra. The first relies on finding a minimum set of sufficiently accurate electronic surfaces. The second increases the time step required for convergence of exact quantum simulations by using different split-step algorithms to solve the time-dependent Schrödinger equation. The third approach lowers the number of trajectories needed for convergence of approximate semiclassical dynamics methods.

Keywords: Pump-probe · Quantum dynamics · Semiclassical approximation · Split-operator method · Stimulated emission

1. Introduction

Typical chemical reactions occur on the femtosecond (fs) time scale. In order to understand the reaction process in detail, one needs to observe it with a femtosecond time resolution. Once a femtosecond time-resolved spectrum is obtained, however, it is often nontrivial to translate the spectrum into a picture of the quantum dynamics (QD) occurring during the reaction. For a theorist, on the other hand, the dynamical picture is frequently the starting point. While the time-dependent picture is extremely useful even for understanding continuous wave spectra,[1] for time-resolved spectra it is obviously a natural choice. Instead of inferring the dynamics of the system from the measured spectra, the theorist does exactly the opposite: he or she computes the QD first and converts it to a time-resolved spectrum later. The main problem is the calculation of a certain time-correlation function; the spectrum is then obtained easily by a Fourier transform. For example, for the pump-probe stimulated emission spectrum, within the electric dipole approximation, time-dependent perturbation theory, and for ultrashort pulse length, the correlation function of interest is given by Eqn. (1):

$$C_{\text{st.em.}}(t,\tau) = E_{pu}^2 E_{pr} Tr[\rho_0(T)\mu_{01}U_1(-t-\tau)\mu_{10}U_0(t)\mu_{01}U_1(\tau)\mu_{10}],$$
$$U_j(t) = \exp(-iH_j t/\hbar). \quad (1)$$

Here E_{pu} and E_{pr} are the amplitudes of the pump and probe pulses, $\rho_0(T)$ is the nuclear density operator in the electronic ground state at temperature T, U_j is the quantum (QM) evolution operator for the nuclei on the j^{th} surface, μ_{ij} is the dipole moment between states i and j, τ is the time delay between the pump and probe pulses, and t is time after the probe pulse. In order to focus on (and enhance) the QD nature of the problem, let us assume $T = 0$. Adopting the Franck-Condon approximation, the correlation function (1) becomes $C(t, \tau) = (E_{\text{pu}})^2 E_{\text{pr}} |\mu_{10}|^4 f(t, \tau)$ where the so-called 'fidelity' amplitude is

$$f_{\text{st.em.}}(t,\tau) = \langle\psi_0|U_1(-\tau)U_1(-t)U_0(t)U_1(\tau)|\psi_0\rangle, \quad (2)$$

and ψ_0 is the vibrational ground state on the ground electronic surface. The time-resolved stimulated emission spectrum is given by the Fourier transform

$$\sigma_{\text{st.em.}}(\omega,\tau) \propto \int_{-\infty}^{\infty} f_{\text{st.em.}}(t,\tau)e^{i\omega t}dt. \quad (3)$$

Below, we will not consider the contribution to the pump-probe spectrum from the ground-state absorption (or 'bleach'), which can be computed from Eqn. (2) by exchanging the roles of ground and excited surfaces during the dynamics. While playing a role in the pump-dump-pump-probe experiment we shall analyze below, the bleach is independent of the delay time for the strict pump-probe experiment, in which the initial state is stationary, and hence can be subtracted from the time-resolved spectrum. Note that a general pulse shape, nonperturbative effects, and non-Franck-Condon transitions can be included similarly as nonadiabatic couplings discussed below. The finite temperature effects can be treated *via* averaging with a QM Boltzmann factor, using for example, path integral Monte Carlo or path integral molecular dynamics methods that are used in our group for computing thermal rate constants and isotope effects.[2] The hardest part, however, remains, namely the calculation of the time-dependent state of the system, *i.e.* solving the time-dependent Schrödinger equation (TDSE),

$$i\hbar\frac{\partial}{\partial t}|\psi(t)\rangle = H|\psi(t)\rangle, \quad (4)$$

or, more generally, the Liouville-von Neumann equation for the density operator.

There are two general ways to solve the TDSE. One can either solve it numerically exactly, which unfortunately scales exponentially with the number (D) of QM degrees of freedom, or use an approximation that scales favorably with D and hope that the approximation is good enough for the given system. In both cases, the calculations are usually much more expensive than *e.g.* molecular dynamics, and so one

*Correspondence: Prof. J. Vaníček
Ecole Polytechnique Fédérale de Lausanne
Institut des Sciences et Ingénierie Chimiques
Laboratory of Theoretical Physical Chemistry
EPFL SB ISIC LCPT, BCH 3110
CH-1015 Lausanne
Tel.: +41 21 693 47 36
Fax: +41 21 693 97 55
E-mail: jiri.vanicek@epfl.ch

has to compromise between the accuracy of the method and its efficiency.

In this article, we will explore three specific approaches for speeding up the calculation of time correlation functions needed for time-resolved electronic spectra: The first relies on a choice of a minimum set of sufficiently accurate electronic surfaces. The second approach increases the required time step in exact simulations by using different split-step algorithms to solve the TDSE. The third approach lowers the number of trajectories needed for convergence of approximate semiclassical (SC) dynamics methods.

2. Finding a Minimum Set of Sufficiently Accurate Electronic Surfaces

Before starting a QD calculation, one has to decide how many coupled electronic potential energy surfaces (PESs) to include in the calculation and choose an appropriate method to compute these surfaces as well as nonadiabatic or spin-orbit couplings between them. The ability to find a minimum number of sufficiently accurate surfaces is the first important contribution to the efficiency of a QD simulation.

The calculation of PESs can be done either beforehand or 'on the fly', *i.e.* simultaneously with the QD. The surfaces and couplings must be accurate enough, yet not too expensive since the QD itself is very expensive. However, it is very difficult to predict the effect of the accuracy of a PES on the QD without performing the QD itself. In our group, we have found an efficient SC method that can do exactly this.[3] The accuracy at time t is defined as the QM fidelity $F(t) = |f(t)|^2$, *i.e.* the squared fidelity amplitude or the overlap of the time-dependent wave functions propagated on the accurate (but expensive) and approximate (yet cheap) surfaces. The fidelity is evaluated with a SC approximation, called dephasing representation (DR)[4] which only requires running classical dynamics on the approximate surface (and some potential, but not force evaluations on the accurate surface).

Knowing how to balance accuracy and efficiency for a given PES, one must further decide how many coupled PESs to include in the calculation. Including additional PESs makes the calculation more accurate but also much more expensive. Moreover, the importance of additional surfaces depends on the dynamics (in particular, on the initial condition): so in principle, one would have to perform the QD on many coupled surfaces to determine which surfaces are needed for the dynamics. It turns out that there is a simple way to estimate the dynamical importance of nonadiabatic (or spin-orbit or diabatic) couplings between PESs, using the DR of QM fidelity.[5] For example, the significance of nonadiabatic couplings is measured by 'nonadiabaticity', *i.e.* fidelity defined as the overlap between the wave functions propagated using the uncoupled Born-Oppenheimer Hamiltonian and the fully coupled Hamiltonian.[6]

3. Accelerating Quantum Dynamics with High Order Split Operator Methods

Once the choice of PESs has been made, the numerically exact QD can be performed on either a fixed or moving grid. The moving grid approaches, such as the multi-configuration time-dependent Hartree method (MCTDH),[7] allow the treatment of a higher number of degrees of freedom, but it is more difficult to estimate rigorously their errors.[8] Here we focus on fixed-grid methods.

If the QM state $|\psi(t)\rangle$ at time t is known, the state at time $t + \Delta t$ is computed as

$$|\psi(t+\Delta t)\rangle = e^{-iH\Delta t/\hbar}|\psi(t)\rangle. \quad (5)$$

One way to increase the time step Δt in a simulation without sacrificing the accuracy is to realize that the TDSE (4) is not *any* differential equation, but a very specific one with many nice properties, such as time-reversibility, unitarity (the norm of the wave function is preserved under time-evolution), and symplecticity (a somewhat technical generalization of unitarity).[8] A method that preserves these properties is more likely to remain accurate with a longer time step Δt. Among such methods are the so-called split operator methods[9]

$$e^{-i\Delta t H/\hbar} = \prod_{j=1}^{n} e^{-ia_j \Delta t V/\hbar} e^{-ib_j \Delta t T/\hbar} + O(\Delta t^{m+1}), \quad (6)$$

where V is the potential energy, T is the kinetic energy, and m is the order of the method. For real a_j, b_j, all such methods are automatically symplectic and unitary since both the kinetic and potential propagations themselves are. If the splitting (6) is also symmetric, then the method is time-reversible. Below we implement and compare several such methods.

The simplest method, a discrete-time implementation of the Lie-Trotter formula,[10] is the *first order split operator* (SO1) algorithm ($n = 1$, $a_1 = 1$, $b_1 = 1$), which is however not time-reversible. The algorithm works as follows:

i) wave function in position representation is Fourier-transformed to momentum representation in which T is diagonal [with the cost O(n log n), where n is the dimension of the Hilbert space representing the state],
ii) kinetic propagation is trivially done by multiplication [with a cost O(n)],
iii) momentum wave function is inverse-Fourier-transformed back to the position representation in which the potential is diagonal [cost O(n log n)],
iv) potential propagation is done by multiplication [cost O(n)].

For this as well as other algorithms, the most expensive part is the Fast Fourier Transform (FFT), and so the cost of an algorithm for a given Δt is estimated by the number of FFTs. The SO1 algorithm requires two FFT operations ($f = 2$) and it is of first order in Δt ($m = 1$).

An improved algorithm is the *second order split operator* (SO2) algorithm[9a] ($n = 2$, $a_1 = a_2 = ½$, $b_1 = 1$, $b_2 = 0$, $f = 2$, $m = 2$) which requires also only two FFTs, but is accurate to second order in Δt. It is possible to design algorithms of any order, but they become increasingly complicated and beyond fourth order are rarely used. Hence we consider three types of fourth order split-operator algorithms that differ significantly in their design. The most straightforward one is an algorithm with all *real coefficients* [SO4-R, $n = 4$, $a_1 = a_4 = \alpha / 2$, $a_2 = a_3 = \alpha (1 - 2^{1/3})/2$, $b_1 = b_3 = \alpha$, $b_2 = -2^{1/3} \alpha$, $b_4 = 0$ where $\alpha = (2 - 2^{1/3})^{-1}$, $f = 6$, $m = 4$].[9b,9c,9g] While this is an optimal fourth order algorithm (*i.e.* an algorithm minimizing f) with all real coefficients, one can lower the number of the FFT operations by either considering complex coefficients or by allowing commutators of T and V in the splitting defined by Eqn. (6).

The former approach starts with a 3rd order algorithm with *complex coefficients* [SO3-C, $n = 3$, $a_1 = a_3^* = \beta / 4$, $a_2 = ½$, $b_1 = b_2^* = \beta / 2$ where $\beta = 1 + 3^{-1/2}\, i$, $f = 4$, $m = 3$],[9e,9f] which unfortunately is not strictly unitary. The order is increased by concatenating the SO3-C algorithm for odd steps with its conjugate algorithm SO3-C* for even time steps, resulting in the 4th order algorithm SO4-C. The error is measured by the norm of the difference of the approximate and exact wave functions. [If the error is only measured by the (less stringent) overlap of the two wave functions, the 4th order can be reached simply by renormalizing the wave function after each step of the SO3-C algorithm.[9f]]

The latter approach generalizes the splitting by permitting the exponential of the commutator

$$[V,[T,V]] = \sum_i \frac{\hbar^2}{m_i}(\nabla_i V)^2 \quad (7)$$

in the splitting (6). An optimal resulting algorithm, requiring only four FFTs, is an

algorithm with the *gradients* of V (SO4-G, $n = 3, f = 4, m = 4$).[9d,11]

$$e^{-i\Delta t H/\hbar} = e^{-i\frac{1}{6}\Delta t V/\hbar}\, e^{-i\frac{1}{2}\Delta t T/\hbar}\, e^{-i\frac{2}{3}\Delta t V_{\mathrm{eff}}/\hbar}\, e^{-i\frac{1}{2}\Delta t T/\hbar}\, e^{-i\frac{1}{6}\Delta t V/\hbar} + O(\Delta t^5),$$
$$V_{\mathrm{eff}} = V - \frac{1}{48}\left(\frac{\Delta t}{\hbar}\right)^2 [V,[T,V]]. \qquad (8)$$

4. Semiclassical Dynamics for Time-resolved Spectroscopy

An alternative approach to speeding up QD calculations is to use SC dynamics. While not exact, SC methods can approximately describe all types of QM effects, such as interference, coherence, tunneling, zero-point energies, *etc*. This distinguishes SC dynamics from classical molecular dynamics that describes the motion of nuclei purely classically even though it may use *ab initio* quantum chemistry methods to compute the electronic PESs.

All SC methods use classical trajectories, but in addition attach phase information to each trajectory. When contributions of various trajectories are added up, this phase permits interference effects, absent in purely classical dynamics. A SC wavefunction can be generally written as

$$\psi(q,t) = \sum_j A_j e^{i\phi_j}, \qquad (9)$$

where the sum runs over classical trajectories j, A_j is the square root of classical probability to be at point q at time t, and ϕ_j is the corresponding phase. As a result, SC dynamics resembles very much geometrical optics, making QM phenomena more intuitively understandable.

A starting point in all SC methods is the so-called Van-Vleck-Gutzwiller propagator[12] describing the probability amplitude to get from point q' to point q'' in time t. This propagator is hard to use in practice because in many-dimensional systems it is very difficult (and expensive) to find all classical trajectories from q' to q'' in time t. A clever solution was provided by Miller's initial value representation that transforms this boundary value problem to an initial value problem which is much easier to solve.[13] One has to sample the initial coordinates and momenta from a distribution in phase space describing the initial QM state, run trajectories, and at time t compute the wave function using a formula similar to Eqn. (9).

Here we focus on four SC initial value methods that provide extensions to Miller's idea by applying it to the coherent states, *i.e.* Gaussian wave packets (GWPs).[14] The propagated GWPs smooth out wild oscillations in the Van Vleck-Gutzwiller propagator and, as a consequence, GWPs lead to faster convergence. All four methods can be written in the same general form that describes the overlap of an initial GWP g_{x_i} centered at x_i with a final GWP g_{x_f} centered at x_f,

$$\left\langle g_{x_f} \middle| e^{-iHt/\hbar} \middle| g_{x_i} \right\rangle = h^{-D} \int d^D x^0\, C(x^0,t) R(x^0,t) e^{iS(x^0,t)/\hbar}, \qquad (10)$$

where $S(x^0,t)$ is the classical action at time t along a trajectory starting at a phase space point $x^0 = (q^0, p^0)$ and ending at point x^t, and C and R are factors depending on the method. In the original *Frozen Gaussian Approximation* (FGA),[14a] the C and R factors are the simplest possible,

$$C_{\mathrm{FGA}}(x^0,t) = \left\langle g_{x_f} \middle| g_{x^t} \right\rangle \left\langle g_{x^0} \middle| g_{x_i} \right\rangle,$$
$$R_{\mathrm{FGA}}(x^0,t) = 1. \qquad (11)$$

In words, the FGA covers the initial state with GWPs, propagates their centers to time t while neglecting their spreading (*i.e.* Gaussians are 'frozen' like snowballs[14a]), computes the action along each trajectory, and averages the phase factor exp ($iS/\hbar$) over the trajectories. While the FGA is remarkably simple and works surprisingly well, it can be improved in two ways: First, Herman and Kluk corrected the R factor to get a more accurate and, in fact, uniform SC approximation called the *Herman-Kluk* (HK) *propagator*, in which R depends on the classical stability matrix.[14c] Second, the convergence of the FGA can be sped up by smoothing the frozen Gaussians *via* (who could have guessed?) new Gaussians. This procedure modifies the C factors and results in the *cellular dynamics* (CD).[14b] Both ideas were used simultaneously in the *cellularized Herman-Kluk* (CHK) *propagator*, originally called *cellularized frozen Gaussian approximation*,[14d] which is both the most accurate (due to improved R) and the most efficient (due to improved C) of the four methods.

Finally, we will compute the correlation function $f(t, \tau)$ and the time-resolved stimulated emission spectrum using the DR of fidelity, a SC method used by one of the authors to measure the sensitivity of QD to perturbations.[4a] In the present setting,

$$f_{\mathrm{DR}}(t,\tau) = h^{-D} \int dx^0 \rho_W(x^0) \exp\left(\frac{i}{\hbar}\int_\tau^{\tau+t} dt' \left(V_1(q') - V_0(q')\right)\right) \qquad (12)$$

where ρ_W is the Wigner-Weyl transform of the initial state and V_j is the j^{th} PES. Each trajectory $x^{t'}$ is propagated on the excited PES V_1 for time τ and subsequently on the average PES $(V_0 + V_1)/2$ for time t. The method is analogous to the phase averaging of Mukamel[15] which has been previously used for computing transient absorption spectra by several authors.[16]

5. Results and Discussion

5.1 *The System*

For numerical tests we chose a two-dimensional system describing the vibrational dynamics of a collinear NCO molecule. Li *et al.*[17] give an analytical fit to the *ab initio* data for the $X^2\Pi$ ground and $A^2\Sigma^+$ excited electronic states, where the NC and CO bond lengths are confined to the interval [2.0–2.6] a.u. In the SC approach it was necessary to have the potential defined on a larger domain and we have thus used an approximate fit to this potential by a sum of two Morse terms defined in the bond-length coordinates r_j as

$$V(r_1,r_2) = V_0 + \sum_{j=1,2} D_j \cdot \left(1 - \exp(-\beta_j \cdot (r_j - R_j))\right)^2, \qquad (13)$$

and coupled *via* the kinetic term. The fitted parameters (atomic units are used throughout this paper) are listed in Table 1. In mass-scaled normal mode coordinates and within the harmonic approximation, the ground vibrational state of the $X^2\Pi$ surface is a single GWP with the widths equal to 14.44 and 10.35. The exact ground state was found by imaginary-time propagation[18] of the above-mentioned GWP. In numerical tests, this exact ground state was approximated by

fitting to a Gaussian form, which resulted in slightly different widths, namely 14.55 and 10.43. For calculation of the pump-probe spectra, a nonstationary initial state was generated by a pump-dump technique,[19] in which the original state was promoted to the upper surface, propagated there for a net time of 520 a.u., dumped to the lower surface, and propagated there for additional 480 a.u. The shape of the resulting wavepacket resembled again a single shifted GWP[20] to which it was fitted.

5.2 *Efficiency of Various Split-operator Methods*

Before showing the time-resolved spectra, we compare the efficiency of the various split-operator methods. Besides the number of FFTs, the efficiency is determined predominantly by the size Δt of the time step that introduces a fixed discretization error (determined, *e.g.*, by machine precision) to the wavefunction after each step. The faster a propagation method converges, the larger the time step can be chosen. Fig. 1 shows the error of the wavefunction propagated for time $t = 128$ a.u. on the $A^2\Sigma^+$ PES as a function of Δt for different split operator algorithms. The error is defined as $\|\psi_{\Delta t}(t) - \psi_0(t)\|$ where $\psi_0(t)$ is the benchmark wavefunction propagated with the same method and a very small time step of 2^{-9}, *i.e.* 0.00195 a.u.

Fig. 1 shows that the complex propagation schemes SO3-C and SO4-C are unstable for time steps larger than 6.4 and 4 a.u., respectively, due to the non-unitary propagation.[9f] A rough estimate on the maximal time step size can be deduced from the near-unitarity condition on the kinetic evolution operator U_T. Employing the Heisenberg uncertainty relation, the maximal momentum is related to the grid spacing Δq as $p_{max} \leq \pi \hbar / \Delta q$.
In order for U_T to be almost unitary, the time step Δt has to fulfill the condition

$$\Delta t < \frac{2m\Delta q^2}{\pi^2 \hbar \operatorname{Im} z}, \qquad (14)$$

where z is the complex splitting constant. The denser the grid in coordinate space, the larger the maximal phase in the kinetic term, and the smaller the maximal Δt for complex splitting propagation. For a grid spacing of 4 a.u. in each dimension Δt has to be smaller than 22 a.u. which corresponds to the actual behavior of the SO4-C and SO3-C methods. The earlier breakdown of the SO4-C method is due to the combined effect of the last and the first splitting step of each time step, resulting in a larger effective time step.

Incidentally, for very dense grids, the 4th order splitting with real coefficients (SO4-R) also runs into difficulties by effectively exhibiting second order behavior. The culprit could be related to the numerical issues resulting from large phase factors in the kinetic evolution operator following again directly from the uncertainty relations. Finally, in the opposite case of a very *low* grid density, the predicted 4th order convergence of SO4-G deteriorated to the 2nd order. To conclude, high order methods can result in much smaller errors and a much higher efficiency, but they must be used with great care as the errors depend strongly on the grid spacing.[8]

Table 1. Parameters (in a.u.) of the approximative potential fit from Eqn. (12)

	R_1	R_2	D_1	D_2	β_1	β_2	V_0
$X^2\Pi$	2.302	2.246	0.1273	0.1419	1.414	1.718	–167.653
$A^2\Sigma^+$	2.234	2.232	0.1432	0.1417	1.516	1.816	–167.548

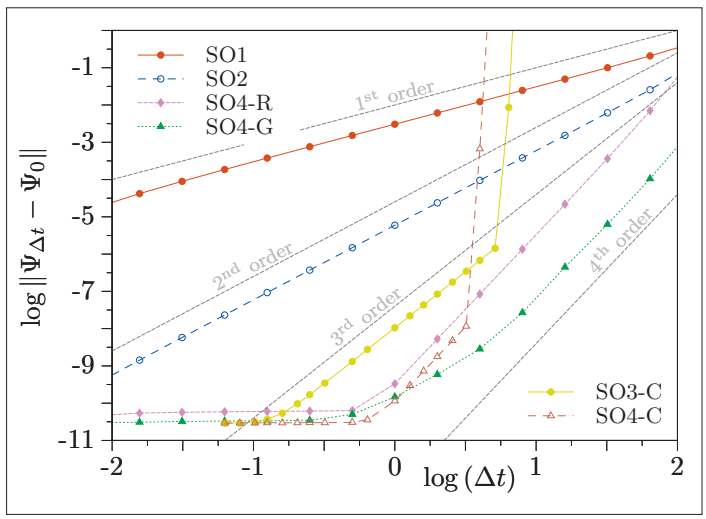

Fig. 1. Error of the quantum wave function (at time t = 128 a.u.) as a function of the time step Δt (in a.u.) for various split-operator methods.

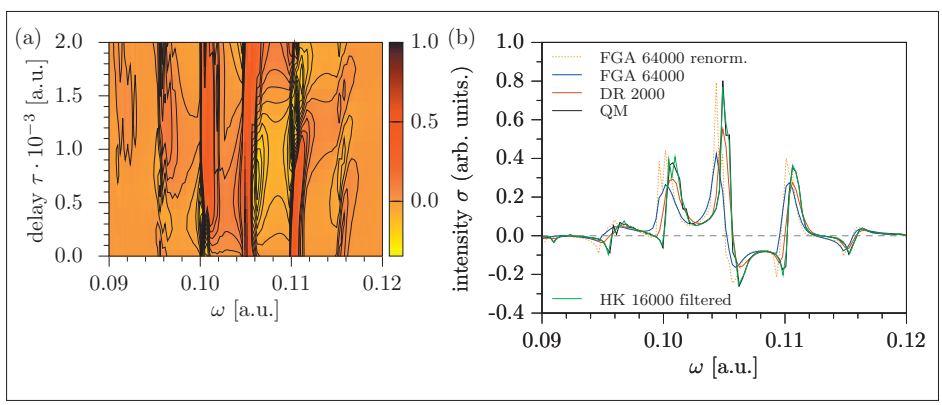

Fig. 2. Pump-probe stimulated emission spectra: (a) Quantum results (contours are plotted for intensities from –0.34 to 0.2 at intervals of 0.04). (b) Semiclassical results for the delay time of 300 a.u. [the number of trajectories used is shown after the name of the approximation].

5.3 *Time-resolved Spectra and Correlation Functions*

Numerical tests consisted in the computation of the correlation function and transient spectrum, *i.e.* quantities defined in Eqns. (2) and (3), where U_0 and U_1 denote the evolution operators corresponding to the $X^2\Pi$ and $A^2\Sigma^+$ electronic states, respectively. Panel (a) of Fig. 2 depicts the resulting benchmark QM transient stimulated emission spectra[21] calculated using the 4th order split operator method SO4-R with a time step Δt = 5 a.u. Prior to the actual spectra calculation by the Fourier transform (3), the correlation function (2) was damped[14d] by a Gaussian decay function $\exp(-t^2/T^2)$ with T set to 10^4 a.u. (see Fig. 3).

Panel (b) of Fig. 2 compares QM and converged SC spectra computed at a specific delay time τ of 300 a.u. All SC calculations used a SC symplectic integrator that we have designed based on Chin's 4th order classical symplectic integrator utilizing force gradients.[11] Chin's integrator, in turn, is a classical analog of the QM propagator SO4-G.

The original FGA method reproduces the spectrum at least qualitatively; nev-

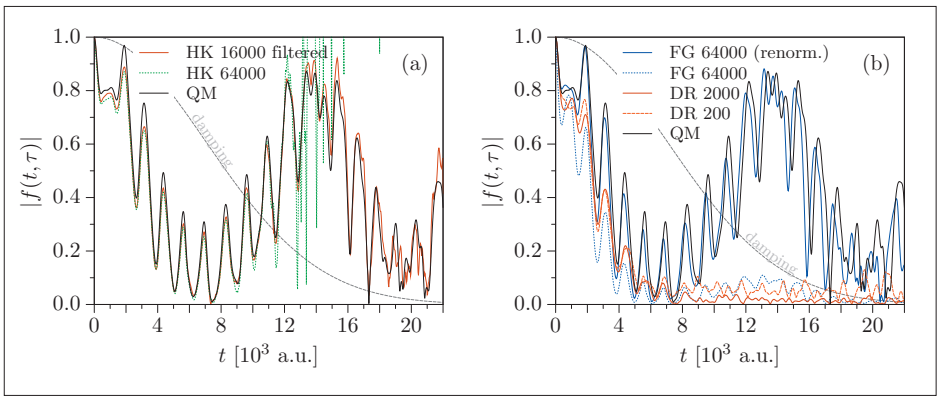

Fig. 3. The magnitude of the time-dependent correlation function as a function of time computed with various SC methods. [The number of trajectories used is shown after the name of the method.] (a) The slow convergence of the HK method can be remedied by heuristic filtering out of trajectories with exponentially growing prefactors. (b) The improvement of the FGA by renormalization and the fast convergence of the DR. [The displayed correlation functions were multiplied by the damping function (shown by a dashed gray curve) in order to obtain finite-resolution spectra in Fig. 2.]

ertheless it is improved by a repeated renormalization of the correlation function f [see Fig. 2(b)]. While the HK method with filtering (to be explained below) gives almost exact spectrum, the DR spectrum is reasonably accurate yet converges with much fewer trajectories.

A stringent criterion on the accuracy of various SC methods is the undamped correlation function $f(t, \tau)$; its absolute value squared is shown in Fig. 3. In agreement with conclusions made by Kay as well as Walton and Manolopoulos,[14d,22] we observed that the convergence of the HK is significantly slowed down by just a few trajectories the prefactor of which grows exponentially fast in time [see Fig. 3(a)]. We were unable to obtain sensible results based on the implementation of the original HK method for times larger than, roughly, 10^4 a.u. Similar observation led Walton and Manolopoulos to the introduction of the CHK method mentioned above.[14d] Nevertheless, as pointed out by Kay,[22a] even a much simpler heuristic approach, consisting in a repeated elimination of trajectories with the largest prefactors, can lead to reasonable results. Fig. 3(a) supports this claim: The green dashed line represents HK results for 64000 trajectories whereas the solid red line corresponds to the 'filtered HK' results obtained using this heuristic procedure with just 16000 trajectories (fewer than 1% of the trajectories had to be discarded). Finally, Fig. 3(b) compares the FGA and the DR with the QM result. Once again, the renormalization greatly improves the FGA. Unlike the filtered HK method and renormalized FGA, the DR cannot unfortunately describe the recurrence of $|f(t,\tau)|$ after 8000 a.u. However, this should not matter at finite temperature or in the condensed phase where the magnitude of the recurrence will be greatly diminished due to the coupling to the environment, and its effect on the spectrum will be very small. This was already demonstrated by Fig. 2(b), where the spectra were computed from damped correlation functions. We should also highlight the computational efficiency of the DR which, unlike the HK method, does not require the Hessian of the potential, and, moreover, as can be seen in Fig. 3(a), converges with much fewer trajectories than both the FGA and the HK method. In fact, the work in our group has demonstrated that under quite general assumptions, the number of trajectories required in the DR is independent of dimensionality.[23] Finally, we currently work on speeding up the DR even further, using ideas similar to those behind the CD or CHK propagator.

6. Conclusion

In conclusion, we have presented, analyzed, and compared various approaches to speed up the QD calculation of ultrafast time-resolved spectra.

Acknowledgements

This research was supported by the NCCR Molecular Ultrafast Science and Technology (MUST), by SNSF grant No. 200021-124936, and by EPFL.

Received: March 2, 2011

[1] E. J. Heller, *Acc. Chem. Res.* **1981**, *14*, 368.
[2] a) M. Buchowiecki, J. Vaníček, *J. Chem. Phys.* **2010**, *132*, 194106; b) T. Zimmermann, J. Vaníček, *J. Chem. Phys.* **2009**, *131*, 024111; c) T. Zimmermann, J. Vaníček, *J. Mol. Mod.* **2010**, *16*, 1779.
[3] a) B. Li, C. Mollica, J. Vaníček, *J. Chem. Phys.* **2009**, *131*, 041101; b) T. Zimmermann, J. Ruppen, B. Li, J. Vaníček, *Int. J. Quant. Chem.* **2010**, *110*, 2426.
[4] a) J. Vaníček, *Phys. Rev. E* **2004**, *70*, 055201; b) J. Vaníček, *Phys. Rev. E* **2006**, *73*, 046204.
[5] T. Zimmermann, J. Vaníček, *J. Chem. Phys.* **2010**, *132*, 241101.
[6] T. Zimmermann, J. Vaníček, **2011**, unpublished.
[7] H.-D. Meyer, F. Gatti, G. A. Worth, 'Multidimensional Quantum Dynamics: MCTDH Theory and Applications', Wiley-VCH: Weinheim, **2009**.
[8] C. Lubich, 'From Quantum to Classical Molecular Dynamics: Reduced Models and Numerical Analysis', 12 ed., European Mathematical Society, **2008**.
[9] a) M. D. Feit, J. A. Fleck, A. Steiger, *J. Comput. Phys.* **1982**, *47*, 412; b) E. Forest, R. D. Ruth, *Physica D* **1990**, *43*, 105; c) H. Yoshida, *Phys. Lett. A* **1990**, *150*, 262; d) M. Suzuki, *Phys. Lett. A* **1995**, *201*, 425; e) A. D. Bandrauk, E. Dehghanian, H. Lu, *Chem. Phys. Lett.* **2006**, *419*, 346; f) T. Prosen, I. Pižorn, *J. Phys. A: Math. Gen.* **2006**, *39*, 5957; g) M. Suzuki, in 'Computer Simulation Studies in Condensed-Matter Physics', Eds. D. P. Landau, K.-K. Mon, H.-B. Schüttler, Springer: Berlin, **1995**, Vol. VIII; pp 169.
[10] H. F. Trotter, *Proc. Amer. Math. Soc.* **1959**, *10*, 545.
[11] S. A. Chin, *Phys. Lett. A* **1997**, *226*, 344.
[12] M. C. Gutzwiller, *J. Math. Phys.* **1967**, *8*, 1979.
[13] a) W. H. Miller, *J. Chem. Phys.* **1970**, *53*, 3578; b) W. H. Miller, *J. Phys. Chem. A* **2001**, *105*, 2942.
[14] a) E. J. Heller, *J. Chem. Phys.* **1981**, *75*, 2923; b) E. J. Heller, *J. Chem. Phys.* **1991**, *94*, 2723; c) M. F. Herman, E. Kluk, *Chem. Phys.* **1984**, *91*, 27; d) A. R. Walton, D. E. Manolopoulos, *Mol. Phys.* **1996**, *87*, 961.
[15] S. Mukamel, 'Principles of Nonlinear Optical Spectroscopy', OUP USA, **1999**.
[16] a) S. A. Egorov, E. Rabani, B. J. Berne, *J. Chem. Phys.* **1999**, *110*, 5238; b) N. E. Shemetulskis, R. F. Loring, *J. Chem. Phys.* **1992**, *97*, 1217; c) Q. Shi, E. Geva, *J. Chem. Phys.* **2005**, *122*, 064506.
[17] Y. Li, S. Carter, G. Hirsch, R. J. Buenker, *Mol. Phys.* **1993**, *80*, 145.
[18] R. Kosloff, H. Tal-Ezer, *Chem. Phys. Lett.* **1986**, *127*, 223.
[19] R. Baer, R. Kosloff, *J. Phys. Chem.* **1995**, *99*, 2534.
[20] Widths are approximately equal to (15.73,11.08), the centre is shifted by (10.8, 3.1) a.u.
[21] W. T. Pollard, S. Y. Lee, R. A. Mathies, *J. Chem. Phys.* **1990**, *92*, 4012.
[22] a) K. G. Kay, *J. Chem. Phys.* **1994**, *101*, 2250; b) A. R. Walton, D. E. Manolopoulos, *Chem. Phys. Lett.* **1995**, *244*, 448.
[23] C. Mollica, J. Vaníček, **2011**, unpublished.